Fullwave Analysis of Thickness and Conductivity Effects in Coupled Multilayered Hybrid and Monolithic Circuits

M.L. TOUNSI [1], R. TOUHAMI [1], and M.C.E. YAGOUB [2]

[1] Instrumentation Laboratory, Faculty of Electronics and Informatics
U.S.T.H.B University
P.O Box 32, El-Alia, Bab-Ezzouar, 16111, Algiers
ALGERIA
[2] School of Information Technology and Engineering
University of Ottawa
800 King Edward, Ottawa, Ontario, K1N 6N5
CANADA

Abstract: - In this paper, the hybrid-mode spectral domain approach is generalized to describe the dispersion properties of coupled microwave circuits with any arbitrary metallization thickness and finite conductivity in multilayer configuration. The influence of finite metallization thickness on the frequency dependent modal propagation characteristics is shown for both suspended and inverted coupled structures and can be easily extended to any multilayered circuit. The phase constant and effective permittivity with finite strip thickness and finite conductivity are discussed for hybrid and monolithic circuits.

Key-Words: - Hybrid Mode, Electromagnetic Field, Integrated Circuits, Metallization Thickness, Numerical Methods, Spectral Domain Approach.

1 Introduction

Any microwave integrated circuit response like losses, dispersion, noise, etc., depends closely on how the implemented miniaturized devices are modeled. To be efficient, this aspect requires the resolution of many issues related to the complexity of the integrated structure such as the hybrid nature of the electromagnetic (EM) fields. Among these features, edge effects can significantly modify the distribution of the EM fields because of the influence of the metallization thicknesses which role becomes more and more significant as the frequency increases.

Finite metallization thickness is one of the main factors that affect the propagation and attenuation characteristics of planar waveguides, especially in high density miniaturized monolithic microwave integrated circuits (MMICs) used in moderate power purpose or in higher microwave and millimeter-wave frequency bands. As a result of improvements in fabricating high performance complex components in these frequency bands, the design of MMICs requires efficient simulation tools with more accuracy for finite thickness planar transmission lines [1].

This effect can be negligible for single circuit lines even if the circuits are carried out in thick film technology. Nevertheless, this role becomes considerable when the circuits are designed to support high powers, or when the conductor exhibits high losses as in antenna networks, or when the circuits are fabricated in MMIC technology. This is because the strip thickness may be comparable to the strip width.

The characteristics of planar circuits with finite strip thickness and conductivity were discussed using various techniques such as the perturbation technique [2], the fullwave mode-matching methods [3], and the method of lines [4].

However, the perturbation approach is not suitable for MMICs since the skin depth and the strip thickness are in the same order, and the above full-wave methods techniques are time consuming. Therefore, an easier and faster method should be developed to meet the evolution of MMICs. This aspect is particularly crucial for multilayer configurations including MIS structures (metal-insulator-semi-conductor) on GaAs or silicon when the loss factor of the layers needs to be taking into account.

This paper deals with the analysis of the influence of both thickness and finite conductivity in coupled multilayered hybrid /monolithic circuits using the spectral domain method (SDA) through the calculation of the dispersion characteristics (phase constant, effective permittivity and guided wavelength) versus frequency, thickness and finite conductivity of the strips.

2 Problem Formulation

Due to the ease of its formulation and its numerical efficiency, the spectral domain approach [5] is a well-known technique for the computation of planar transmission line circuits. The immittance concept [6] further enhances the preprocessing and computing works for multilayer multiconductor structures. This concept is generalized here to generate the complete expressions of Green's functions under their impedance and admittance form.

The structure under analysis is a general unilateral microwave circuit printed on lossy multilayered isotropic layers whose transverse section is depicted in Figure 1. The conductor strips are characterized by finite thickness t and finite conductivity σ_m. The dielectric layers are of loss factor $\mathrm{tg}\delta_i = \sigma_{di}/\omega\varepsilon_i$, where σ_{di} and ε_i are respectively the conductivity and permittivity of dielectric i. Each dielectric layer is characterized by a complex permittivity defined as $\varepsilon_i^* = \varepsilon_0\varepsilon_{r\,i}(1 - j\,\mathrm{tg}\delta_i)$.

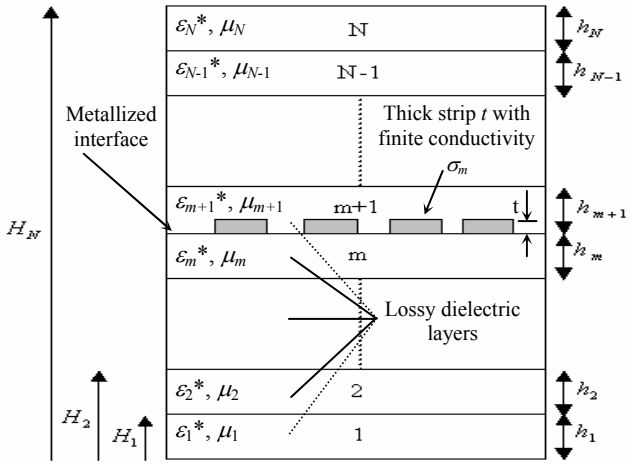

Fig. 1 Section view of a multilayer microwave structure with finite thickness and conductivity.

The modifications made to take into account the thickness effect and finite conductivity of the strips, are based on certain corrective factors with regard to the case of thin metallization (t = 0) and infinite conductivity ($\sigma_m \to \infty$). In order to obtain the dyadic Green's functions of the structure, the proposed process starts with the decomposition of the EM field into TM-to-y and TE-to-y waves by introducing coordinate transforms [6].

The application of boundary conditions at all interfaces of the multilayered structure yields to a set of matrix equations for the impedance Green's functions [7]

$$\begin{bmatrix} \widetilde{E}_{xm} \\ \widetilde{E}_{zm} \end{bmatrix} = \begin{bmatrix} G_{11} & G_{12} \\ G_{21} & G_{22} \end{bmatrix} \begin{bmatrix} \widetilde{J}_x(\alpha_n) \\ \widetilde{J}_z(\alpha_n) \end{bmatrix} \quad (1)$$

These functions link the tangential components of the electric field to those of the currents on the metallized interface.

3 Equivalent surface impedance

Until now, all strips are considered to be of infinite conductivity and of infinitesimal thickness (t = 0). In order to use the same model for thick planar structures, a transformation technique is used to transform the thin conducting film into infinitely thin strip. Since most conducting films are fabricated to be very thin, the width-to-thickness ratio of these films is quite large.

As a result, the tangential electric to magnetic field ratio on the film surface is almost the same as the value of the surface impedance of the conducting film. This feature allows the impedance boundary condition to be used in solving for the transmission characteristics of the conducting microstrip lines.

When we apply the boundary conditions at the metallized interface of the structure in Figure 1, the conducting strip is treated as an impedance sheet, which is characterized by a jump discontinuity in the values of the tangential magnetic field, but not in the electric field. These boundary conditions that exist on the surface of the strip are written as [8]

$$\vec{n} \wedge (\vec{H}_m - \vec{H}_{m+1}) = \vec{J}_s = -\frac{1}{Z_s}\vec{n} \wedge (\vec{n} \wedge \vec{E}_m) \quad (2)$$

$$\vec{n} \wedge (\vec{E}_m - \vec{E}_{m+1}) = 0 \quad (3)$$

where $\vec{n}$ is the normal to the metallized interface. $\vec{E}_m$ and $\vec{B}_m$ represent respectively the electrical and magnetic fields below the impedance sheet, while $\vec{E}_{m+1}$ and $\vec{H}_{m+1}$ refer to the fields above the sheet.

Z_s is the uniform equivalent impedance of the sheet. If the thickness t of the strip is greater than three penetration depths, the surface impedance

$$Z_s = \sqrt{\omega\mu_0 / 2\sigma_m} \qquad (4\text{-a})$$

will adequately represent the boundary conditions for plane waves with σ_m the strip conductivity. If t is less than three penetration depths, a better boundary condition makes use of

$$Z_s = \frac{1}{t\sigma_m}. \qquad (4\text{-b})$$

4 Modified boundary conditions

The application of these new boundary conditions at $y = H_m$ in the Fourier transform domain results in some modifications to the elements of the Green's impedance matrix. Specifically, the diagonal elements of matrix (1) need to be modified to incorporate the complex surface resistance of the superconducting strip as

$$G_{11m} = G_{11} - Z_s \quad \text{and} \quad G_{22m} = G_{22} - Z_s \qquad (5)$$

Thus, (1) becomes

$$\begin{bmatrix} \widetilde{E}_{xm} \\ \widetilde{E}_{zm} \end{bmatrix} = \begin{bmatrix} G_{11m} & G_{12} \\ G_{21} & G_{22m} \end{bmatrix} \begin{bmatrix} \widetilde{J}_x \\ \widetilde{J}_z \end{bmatrix} \qquad (6)$$

A numerical solution to this matrix equation can be obtained by using Galerkin method in the Fourier domain to eliminate the right side. The current elements are expanded in a set of known basis functions which take the edge singularities into consideration leading to a proper current distribution over the strip.

$$J_x = \sum_{p=1}^{P} c_p J_{xp} \quad \text{and} \quad J_z = \sum_{q=1}^{Q} d_q J_{zq} \qquad (7)$$

5 Application of Galerkin technique

After substituting the Fourier transforms of (7) into (6) and taking inner products of the resulting equations with the test functions $J_{xp'}$, $J_{zq'}$ (chosen equal to the basis functions), we obtain a homogenous system of algebraic equations with the $(P + Q)$ unknown coefficients c_p and d_q.

This system can be written as

$$\begin{aligned} \sum_{p=1}^{P} K_{p,q'}^{1,1}(\beta) c_p + \sum_{q=1}^{Q} K_{p,p'}^{1,2}(\beta) d_q = 0 \\ \sum_{p=1}^{P} K_{q,q'}^{2,1}(\beta) c_p + \sum_{q=1}^{Q} K_{q,p'}^{2,2}(\beta) d_q = 0 \end{aligned} \qquad (8)$$

where

$$K_{r,s}^{i,j}(\beta) = \sum_{n} G_{i,j}(\alpha_n, \beta) \widetilde{J}_{xr} \widetilde{J}_{zs}^{*} \quad r, s = p \text{ or } q \qquad (9)$$

and n is the spectral index. The homogeneous system (8) has been obtained via the application of Parseval's identity. It is solved for the propagation constant by setting the determinant of the system equal to zero and by evaluating the roots of the resulting characteristic equation.

6 Numerical results

The dispersion chart is a necessary step to fix the bandwidth of the dominant and higher order modes which are excited at high frequencies. These modes can create radiation losses that must be avoided.

Figure 2 shows the variation of the even and odd mode phase constants versus frequency for a coupled line on GaAs ($\varepsilon_r = 12$) where the conductor is gold ($\sigma_m = 4.10^7$ S/m) and of thickness $t = 0.6\mu m$.

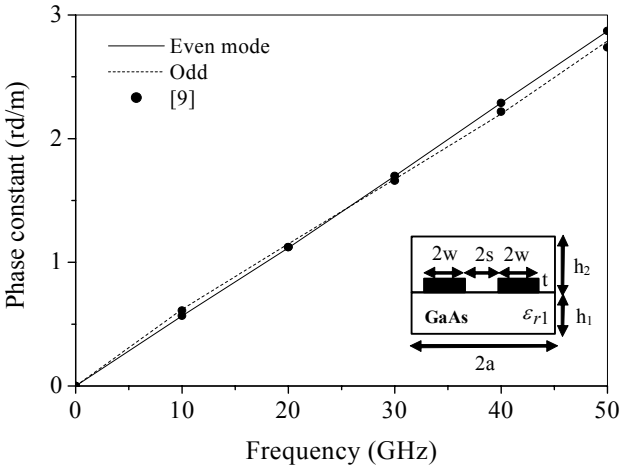

Fig. 2. Even and odd mode phase constant of a shielded coupled microstrip on GaAs substrate; $h_1 = 300\mu m$, $h_2 = 2700\mu m$, $t = 0.6\mu m$, $w = s = 1\mu m$

The losses are essentially due to conducting strips, the even mode which propagates between the strips and ground plane is less attenuated than the odd mode which propagates between the two strips. The even mode is also less dispersive than the odd mode. The obtained results agree well with [9].

Figures 3-a, 3-b, and 3-c, illustrate the variation of the even and odd modes phase constant of a coupled MIS (metal-insulator-semiconductor) structure for different values of the silicon conductivity σ_{Si}.

Contrary to the structures printed on GaAs, the odd and even mode phase constants are different due to the stratified nature of the dielectric layers. When the conductor losses are predominant (for low values of σ_{Si}), the even mode phase constant is greater than the once of the odd mode while for the high values of σ_{Si} (Figure 3.c) we note that beyond 25 GHz it exhibits the inverse behavior and the results are close to those obtained for GaAs. The computed show good agreement with [9]

Figure 4 shows the variation of even and odd modes effective permittivity for coupled planar structures on Silicon for different values of the strip thickness t. Note the decrease of ε_{eff} when t increase for the two propagation modes. Also, we note that the even mode is less dispersive that the odd one. The obtained results agree well with measured data [10].

In Figure 5, the even and odd mode effective permittivities are shown for different combinations of the thickness t and slot width s. In this case, the difference in propagation speeds of the even and odd modes increases as s decrease and the increase is more evident when t is finite, since the two modes are influenced in a different way by t.

Figure 6 gives the characteristics of coupled planar structures in multilayer dielectric configuration. On the contrary, as s decreases, the difference between the even and odd mode speed first increases (for large s) and then decreases. This behavior can be observed only when one takes metallization thickness into account since when $t = 0$ there is a monotone increase in difference of propagation speed. The obtained results agree well with published data [11].

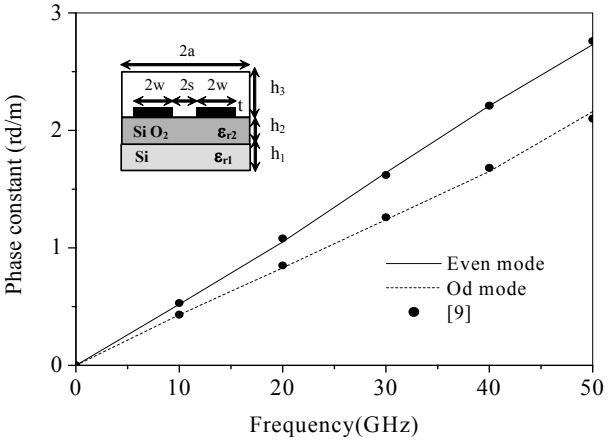

(a) σ_{Si} = 1 S/m

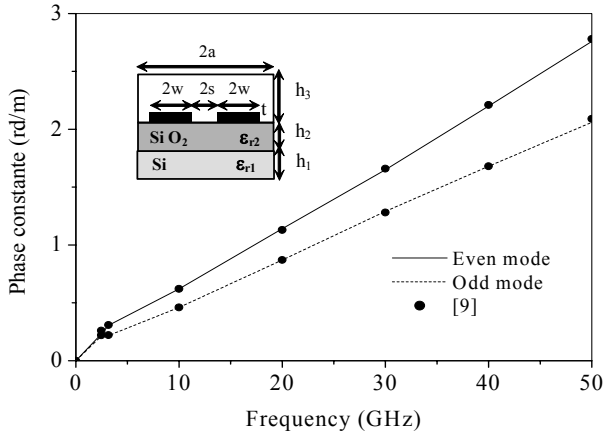

(b) σ_{Si} = 10 S/m

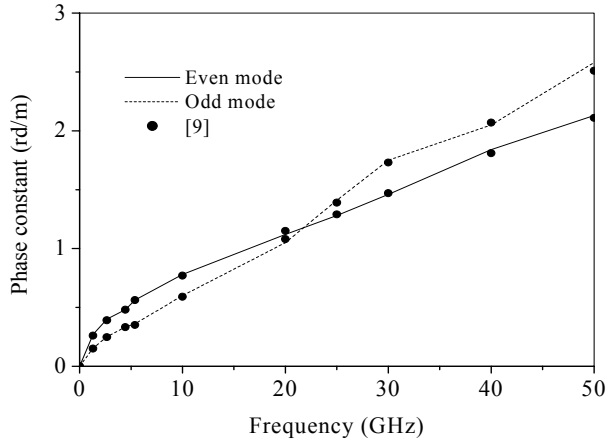

(c) σ_{Si} = 100 S/m

Fig. 3. Phase constant of three-layered coupled planar structures for various values of silicon conductivity (with t = 0.6μm, w = 1μm, $a = h_3/2$, s = 1μm, h_1 = 300μm, h_2 = 0.6μm, $h_3 = 10(h_1+h_2)$, ε_{r1} = 12, and ε_{r2} = 4):
a) σ_{Si} = 1 S/m ; b) σ_{Si} = 10 S/m ; c) σ_{Si} = 100 S/m

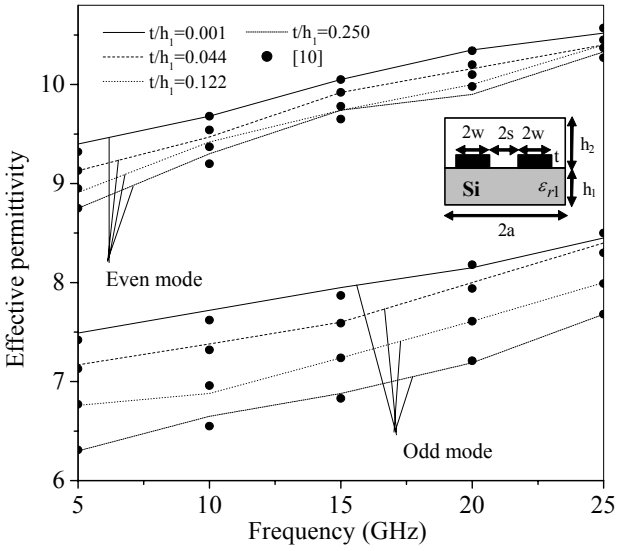

Fig. 4. Effective permittivity versus frequency for various values of strip thicknesses (with $\varepsilon_r = 12.5$, $w/h_1 = s/h_1 = 0.5$, $h_1 = 0.6$mm, $h_2 = 10$mm, and $2a = 13.8$ mm).

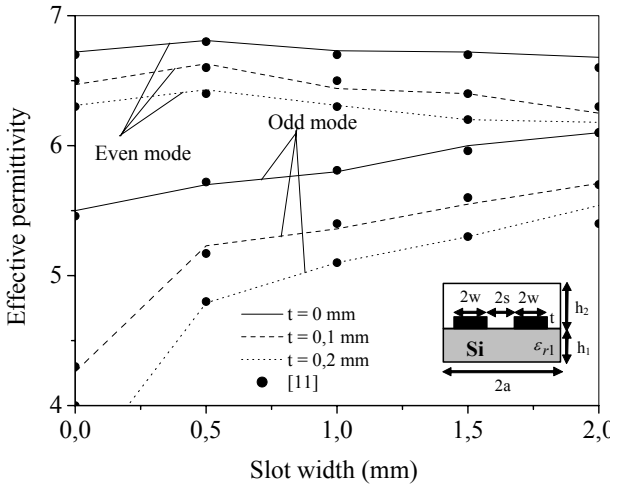

Fig. 5. Effective permittivity versus slot width for different values of strip thicknesses t.

Such behavior is then confirmed for coupled suspended-inverted structures (Figure 7). However, the curves of the effective permittivity exhibit now an inversion of difference in the modal propagation velocity for smaller values of s with respect to the previous case. The obtained results agree well with [11].

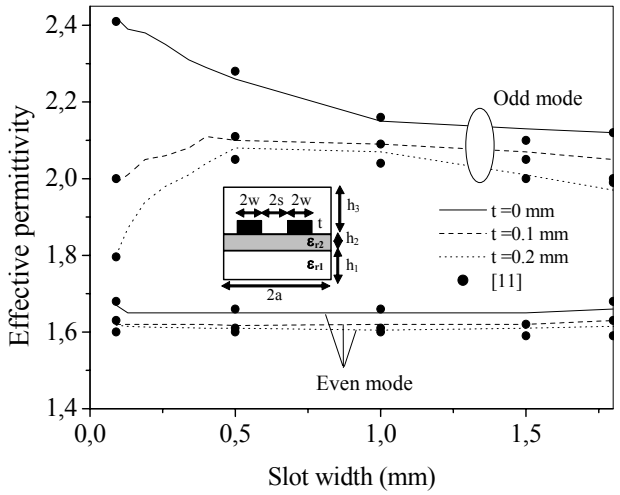

Fig. 6. Effective permittivity versus slot width for different values of t: case of suspended coupled planar structures (with $2a = 10$mm, $w = 0.5$mm, $h_1 = 2$mm, $h_2 = h_3 = 1$mm, $\varepsilon_{r2} = 4$, $\varepsilon_{r1} = \varepsilon_{r3} = 1$).

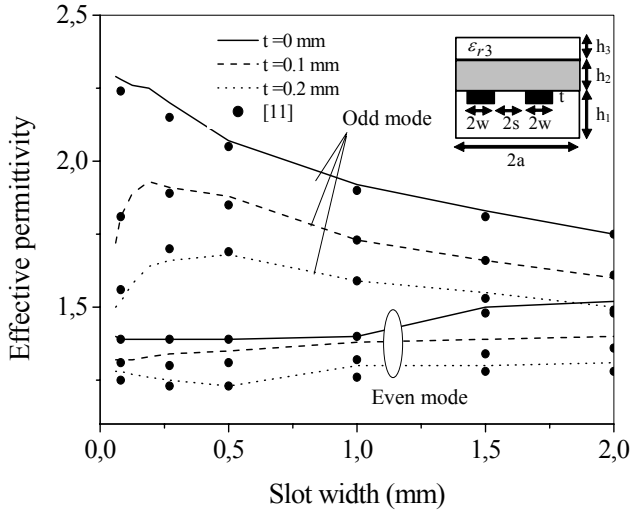

Fig. 7. Effective permittivity versus slot width for different values of thicknesses t: case of inverted coupled planar structures (with $2a = 10$mm, $w = 0.5$mm, $h_1 = 0.5$mm, $h_2 = 1$mm, $h_3 = 3.5$mm, $\varepsilon_{r2} = 4$, $\varepsilon_{r1} = \varepsilon_{r3} = 1$).

7 Conclusion

In this paper, we have proposed an efficient method to analyze the thickness and finite conductivity effects in coupled microwave circuits. The advantage in the CPU time is reflected by the fact that the calculation of phase constant per frequency point does not exceed 1s.

The obtained results show the necessity to taking into account both thickness and finite conductivity of the strips particularly in the case of the MIS lines (metal-insulator-semi-conductor) in the region of slow-wave modes. The dependence of modal phase parallel coupled microstrip on the metallization is significant, especially at higher millimeter-wave frequencies, and for relatively low dielectric constants. The proposed method can be extended to anisotropic structures with superconductor signal strip. Besides, extension to the coplanar strips and coplanar waveguides is straightforward.

References:

[1] Z. Ma, E. Yamashita, and S. Xu, "Hybrid-mode analysis of planar transmission lines with arbitrary metallization cross sections," *IEEE Trans. Microwave Theory Tech*., vol. 41, pp. 491-497, Mar. 1993.

[2] R. A. Pucel, D. J. Mas, and C. P. Hartwig, "Losses in microstrip," *IEEE Trans. Microwave Theory Tech*., vol. 16, pp. 342-350, June 1968.

[3] W. Heinrich, "Full-wave analysis of conductor losses on MMIC transmission lines," *IEEE Trans. Microwave Theory Tech*., vol. 38, pp. 1468-1472, Oct. 1990.

[4] F. J. Schmuckle and R. Pregla, "The method of lines for the analysis of lossy planar waveguides," *IEEE Trans. Microwave Theory Tech*., vol. 38, pp. 1473-1479, Oct. 1990.

[5] T. Itoh and R. Mittra, "A technique for computing dispersion characteristics of shielded microstrip lines," *IEEE Trans. Microwave Theory Tech*., vol. 22, pp. 896–898, Oct. 1974.

[6] T. Itoh, "Spectral domain immittance approach for dispersion characteristics of generalized printed transmission lines, *IEEE Trans. Microwave Theory Tech*., vol. 28, pp. 733–736, July 1980.

[7] M.L. Tounsi, M.C.E. Yagoub, B. Haraoubia, "New design formulas for microstrip transmission lines using high-dielectric substrate," *COMPEL*: *Int J. for Computation and Mathematics in Electrical and Electronic Eng.*, vol. 24, N°1, pp. 15-34, Jan. 2005.

[8] A. I. Amora, H. Ghali, "Full wave analysis of HTS superconducting microstrip transmission lines using spectral-domain immittance approach", *Proc. of 30th National Radio Sci. Conf.,* March 19-21 1996, Cairo, Egypt, pp. 149-156.

[9] H. Jahromi Abiri, *Analyse dynamique des lignes microniques par la méthode spectrale*, Ph.D. thesis, INP Grenoble, France, 1984.

[10] R.T Kollipara, V.K. Tripathi, "Dispersion characteristics of moderately thick microstrip lines by the spectral domain method", *IEEE Microwave Guided Wave letters*, vol. 2, pp. 100-101, Mar. 1992.

[11] G. Gentili, G. Macchiarella, "Quasi-static analysis of shielded planar transmission lines with finite metallization thickness by a mixed spectral-space domain method ", *IEEE Trans. Microwave Theory Tech*., vol. 42, N°2, Feb. 1994.